

25. Marchese, P. J. Variability in the Gulf stream recirculation gyre. *J. Geophys. Res.* **104**, 29549–29560 (1999).
26. Maniatis, T., Fritsch, E. F. & Sambrook, J. *Molecular Cloning. A Laboratory Manual* (Cold Spring Harbor Laboratory Press, Cold Spring Harbor, 1982).
27. Felsenstein, J. PHYLIP (Phylogeny inference package) manual, version 3.5c (Univ. Washington, Seattle, 1993).

## Acknowledgements

We are extremely grateful to the following individuals and organizations for providing the samples used in this study: P. Prouzet, G. Adam, M.-N. de Casamajor, S. L. Jónsdóttir, E. Feunteun, P. Lambert, P. Dumont, C. Briand, R. Leconte, A. Crivelli, C. Gazeau, M.-F. Gazerque, D. Fatin, H. Wickström, A. Yahyaoui, C. Antunes, E. Ciccotti, A. Vøllestad, B. Knights, H. Wilkens and the CEMAGREF. We would also like to thank J. Dodson, M. Castonguay, S. Rogers and J. McNeil for helpful comments on an earlier versions of the manuscript. This work is a contribution to the programme of GIROQ.

Correspondence and requests for materials should be addressed to T.W. (e-mail: wirth\_t@mpiib-berlin.mpg.de).

## Temporal dynamics of a neural solution to the aperture problem in visual area MT of macaque brain

Christopher C. Pack & Richard T. Born

Department of Neurobiology, Harvard Medical School, 220 Longwood Avenue, Boston, Massachusetts 02115, USA

A critical step in the interpretation of the visual world is the integration of the various local motion signals generated by moving objects. This process is complicated by the fact that local velocity measurements can differ depending on contour orientation and spatial position. Specifically, any local motion detector can measure only the component of motion perpendicular to a contour that extends beyond its field of view<sup>1,2</sup>. This “aperture problem”<sup>3</sup> is particularly relevant to direction-selective neurons early in the visual pathways, where small receptive fields permit only a limited view of a moving object. Here we show that neurons in the middle temporal visual area (known as MT or V5) of the macaque brain reveal a dynamic solution to the aperture problem. MT neurons initially respond primarily to the component of motion perpendicular to a contour’s orientation, but over a period of approximately 60 ms the responses gradually shift to encode the true stimulus direction, regardless of orientation. We also report a behavioural correlate of these neural responses: the initial velocity of pursuit eye movements deviates in a direction perpendicular to local contour orientation, suggesting that the earliest neural responses influence the oculomotor response.

If a vertically orientated bar moves up and to the right at a constant velocity, small receptive fields positioned along the length of the contour can measure only the rightward component of motion, as the upward component provides no time-varying information (Fig. 1a). In contrast, cells positioned at the endpoints of the contour can measure motion direction accurately. Since direction-selective cells in the primary visual cortex (V1) have extremely small receptive fields, they are constantly faced with this aperture problem. Moreover, they provide directional input to subsequent stages of visual processing, which could perpetuate errors in motion computation. How are these conflicting motion signals ultimately resolved in the visual cortex? A candidate neural substrate for this computation is the middle temporal visual area (MT or V5), where neurons are known to integrate directional

responses from V1<sup>4</sup>, and are capable of computing motion direction for complex patterns<sup>5–7</sup>.

We used the stimulus illustrated in Fig. 1b to measure neuronal responses in MT of alert macaque monkeys to moving contours at different orientations. Each stimulus consisted of a field of small white bars against a dark background. The size of the bar field was matched to each cell’s classical receptive field. The length of each bar was always 3°, significantly longer than corresponding receptive fields in V1, but smaller than the excitatory receptive fields in parafoveal and peripheral MT<sup>8</sup>. The use of multiple bars ensured that local motion signals from contours and contour endpoints stimulated the MT receptive fields at each instant. (Additional experiments using single long bars yielded results similar to those reported below, but the bar field had the advantage of providing stimulation that was evenly distributed across the receptive field and relatively constant over time.) On each trial, the angle between motion direction and contour orientation ( $\phi$  in Fig. 1a) was 45°, 90° or 135°, and the stimulus moved in one of eight directions. To separate the selectivity of MT cells to static stimulus orientation<sup>9,10</sup> from their directional responses, the stimulus remained stationary for 240 ms before moving. Because the motion direction and relative orientation,  $\phi$ , both varied in intervals of 45°, the orientation did not predict the subsequent motion direction. The preferred direction (PD) for each cell was computed as a vector average of the stimulus direction weighted by the response to that direction. We recorded data from 60 MT cells from three hemispheres in two adult rhesus monkeys.

Figure 2a shows the results from one MT neuron. The earliest direction-selective responses, which occurred at a latency of approximately 70 ms after the onset of stimulus motion, showed a clear dependence on bar orientation relative to motion direction ( $\phi$ ). When the cell was stimulated with a field of bars moving perpendicular to their orientation ( $\phi = 90^\circ$ , red lines), the best responses were obtained for motion down and to the left (PD = 224°). For the  $\phi = 45^\circ$  case (blue lines), the best response occurred for motion to the left (PD = 191°), and in the  $\phi = 135^\circ$  case (green lines), the best response occurred for downward motion (PD = 266°). The effects of contour orientation on the directional responses were highly significant ( $P < 0.001$ , Watson–Williams test), with the peak response always occurring at the same oblique bar orientation (Fig. 2a). These early responses can best be described as encoding the component of stimulus motion perpendicular to bar orientation. We note that they are not responses to orientation

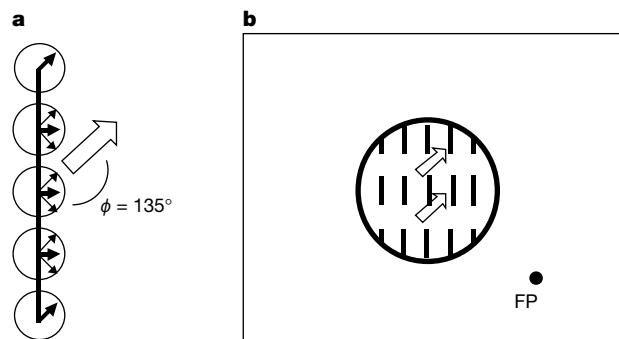


**Figure 1** The aperture problem. **a**, Local motion detectors (indicated by the circles) along the contour can only measure motion perpendicular to the contour’s orientation. For these detectors, the direction of object motion is ambiguous because any of the physical velocities indicated by the thin black arrows would yield the same motion measurement (thick black arrows). The angle between contour orientation and motion direction, as measured clockwise from the motion direction (white arrow), is referred to as  $\phi$ . **b**, The stimulus used in our experiments. A field of bars moved within a window sized to approximate the classical receptive field (depicted by the large circle) of each cell. FP, fixation point.

*per se*: motion up and to the right failed to excite the cell, even though the orientation was optimal. MT responses to static orientation are known to be quite small in amplitude, and so probably would not have directly influenced our results<sup>9</sup>. Figure 2b shows the direction tuning for the same cell when responses are averaged over a 1,500-ms period beginning 500 ms after the onset of stimulus motion. In this case, the best response is always obtained for motion down and to the left, with no statistically significant effect of bar orientation ( $P > 0.2$ , Watson–Williams test). Clearly the initial dependence on bar orientation (Fig. 2a) decreases during the course of prolonged stimulation.

To study the temporal evolution of the shift in MT response properties, we computed the PD for each MT cell in 15-ms bins starting from the earliest direction-tuned responses. These occurred, on average, at 75 ms after the onset of stimulus motion ( $P < 0.05$ , Rayleigh Z-test for deviation from circular uniformity). For each bin, the PD was measured and aligned

relative to the PD computed in the time-averaged  $\phi = 90^\circ$  case. Figure 2c shows the average difference in PDs at each 15-ms bin for the population of 60 MT cells. The earliest responses are highly dependent on stimulus orientation, and this dependence decreases gradually over the course of approximately 60 ms. Within 150 ms after the onset of stimulus motion, MT cells primarily encode the actual stimulus direction, irrespective of orientation. However, there is a slight effect of stimulus orientation on the time-averaged relative PDs (computed in the interval from 500 ms to 2,000 ms after the onset of stimulus motion), resulting in a mean difference of  $-3.1^\circ \pm 16^\circ$  for the  $\phi = 45^\circ$  case and  $5.3^\circ \pm 10.5^\circ$  for the  $\phi = 135^\circ$  case. These small mean differences are nevertheless statistically significant ( $P < 0.05$ , paired one-tailed *t*-test), indicating a slight residual effect of bar orientation on the directional response.

For each cell in our MT population, we also examined the preferred orientation for static bar stimuli, as measured in the 240 ms before the onset of stimulus motion. We found these static bar responses to be quite weak and extremely variable. Moreover, we did not find any consistent relationship between the preferred orientation relative to preferred direction and the temporal properties of the directional response. This was unexpected in light of previous work demonstrating that such orientation preferences are predictive of MT responses to more complex “plaid” stimuli<sup>6</sup>. One possible explanation lies in the fact that previous studies were conducted on anaesthetized animals, whereas our experiments were conducted on awake, behaving animals. We have previously found that, in alert monkeys, the sudden appearance of a stimulus generates a strong response that is not dependent on stimulus features, such as orientation<sup>11</sup>, and this may have weakened the selectivity for orientation. It is also possible that the orientation-selective inputs from V1 are not homogeneous across the MT receptive fields, so that our bar field stimulus activated inputs tuned to many different orientations.

There is strong evidence that MT neurons provide motion signals for the initiation of smooth pursuit eye movements<sup>12–14</sup>. Because pursuit initiation typically occurs approximately 100 ms after the onset of a moving target<sup>15</sup>, the current results predict an orientation-dependent bias in initial eye velocity. To examine this possibility, we trained two monkeys to pursue the centre of a single orientated bar using the same parameters of motion direction and bar orientation as in the physiological recordings. Eye position was monitored with a scleral search coil<sup>16</sup>, and the resulting measurements were used to compute instantaneous eye velocity. We then aligned the eye velocity traces from each trial relative to the actual direction of stimulus motion, and computed the set of median traces across all trials (Fig. 3a). For accurate pursuit movements, eye velocities should match the direction and speed of the target, and indeed this occurs for the  $\phi = 90^\circ$  case (red line). For the  $\phi = 45^\circ$  and  $\phi = 135^\circ$  cases (blue and green lines, respectively), the eye velocity deviates substantially in a direction perpendicular to the orientation of the bar. Note that the recovery of the eye movement from its initial deviation is somewhat slower than the recovery of the MT responses (Fig. 2c). This is likely to be due to differences in the stimuli, which were not equated for speed or bar length. In general the magnitude of the oculomotor effect scaled with bar length, such that the deviation of eye velocity increased monotonically as the size of the bar was varied from  $5^\circ$  to  $25^\circ$ . There was no consistent effect of orientation on eye velocity parallel to the actual direction of stimulus motion (Fig. 3b).

The neural effects of contour orientation on motion integration demonstrated here have a perceptual correlate in humans. It has been shown that the perceived direction of a field of moving bars is initially perpendicular to the orientation of the bars, and rotates towards the actual direction over a period of approximately 200 ms (ref. 17). This time course is somewhat slower than that found for our MT responses, but such a difference is to be expected on the

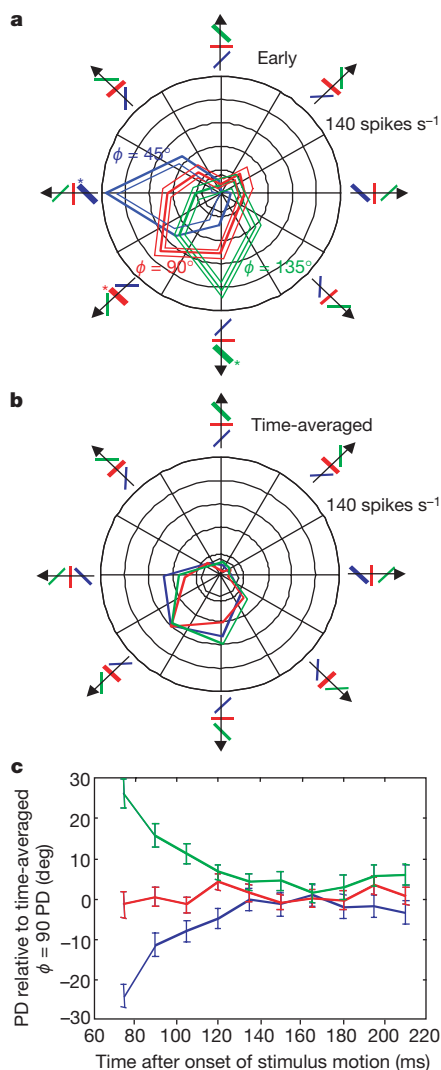


**Figure 2** Evolution of direction tuning. **a**, Earliest direction-tuned response for a single MT neuron. Direction tuning is represented in polar coordinates with axes of stimulus direction (angle) and cell response in spikes per second (radius). Each tuning curve corresponds to a different value of  $\phi$ , which is the angle between bar orientation and motion direction. Thin lines around each tuning curve represent standard error of the mean. **b**, Direction tuning for the same MT cell averaged over the last 1,500 ms of the stimulus presentation. **c**, Directional response as a function of time for the population of 60 MT cells. Error bars indicate standard error of the mean. PD, preferred direction (see text).

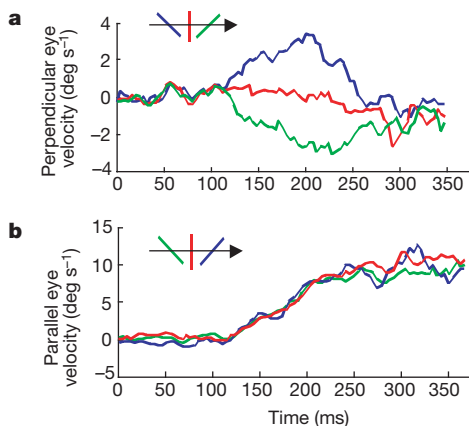


**Figure 3** Visual tracking of an orientated bar. **a**, Median eye velocity perpendicular to the direction of target motion over time for the three bar orientations ( $\phi = 45^\circ, 90^\circ$  and  $135^\circ$ ). **b**, Median eye velocity parallel to the direction of target motion for the same experiments. Error bars (representing standard error of the mean) are smaller than the width of the data lines.

basis of variations in stimulus speed and contrast between the two experiments. For “type II” plaid stimuli, observers initially perceive a vector average of the local motion signals, with the percept subsequently shifting to an intersection of constraints<sup>18</sup>. For these stimuli there is also a residual bias in the perceived direction that is comparable to what we have observed in our time-averaged MT responses<sup>18</sup>. Similarly, human tracking eye movements in response to “barber’s pole” stimuli initially deviate in a direction perpendicular to the orientation of contours, and are subsequently affected by the geometry of the surrounding aperture<sup>19,20</sup>. Taken together, these results suggest that the primate visual system derives an initial estimate of motion direction by integrating ambiguous and unambiguous local motion signals over a large spatial range (at least  $20^\circ$ ), and refines this estimate over time. We have shown that this temporal evolution can be seen at the level of single MT neurons. However, it may also involve neural networks that propagate unambiguous signals to “fill in” the missing information at ambiguous retinal locations<sup>21,22</sup>. Such networks have been the focus of recent neural models that use recurrent<sup>23</sup> or feedback<sup>24</sup> processes to compute motion direction. It is also possible that the visual system computes the motion of contours and contour endpoints via different pathways, with the latter requiring a slightly longer latency<sup>17,25,26</sup>. The present identification of a neural signature for this process should open the door to future experiments to elucidate its mechanism. □

**Methods**

Animals were seated comfortably in a standard primate chair (Crist Instruments) with their heads fixed. They were required to fixate a small red square displayed on a computer monitor at a distance of 57 cm in order to obtain a liquid reward. For physiological experiments, the fixation point was always positioned so that the receptive field was at the centre of the monitor. Stimuli were displayed at a mean luminance of  $0.552 \text{ cd m}^{-2}$ , against a black background (luminance  $0.025 \text{ cd m}^{-2}$ ). Microelectrode recordings were obtained from 60 single units in parafoveal and peripheral MT (mean receptive field eccentricity  $11.1^\circ$ , mean diameter  $12.7^\circ$ ). For physiological experiments, the stimulus consisted of a field of moving bars. Each bar subtended  $3^\circ$  of visual angle, and was centred at a point along an invisible grid, placed approximately in the centre of the receptive field. The spacing between points in the grid was  $5^\circ$  in both the vertical and horizontal directions. The size of the bar field was approximately matched to that of the classical receptive field of each cell. Bars that moved outside the window disappeared, but were replaced with new bars so that the area of stimulation within the receptive field was approximately constant over time. The speed of stimulus motion was also matched to each cell’s preference, as measured with moving dots or bars.

During the physiological experiments, all different stimulus conditions (8 possible directions, 3 possible values of  $\phi$ ) were randomly interleaved. For the earliest directional plot (Fig. 2a), spikes were collected during the interval from 60 to 80 ms after the onset of stimulus motion, and averaged across 10 identical stimulus presentations. The later

responses (Fig. 2b) are averaged across the same 10 stimulus presentations, but include only the last 1,500 ms of the stimulus presentation. For the population data (Fig. 2c), the preferred direction is measured in 15-ms bins and aligned relative to the preferred direction computed in the time-averaged  $\phi = 90^\circ$  case for each cell.

Pursuit experiments were conducted after physiology experiments. On each trial, a bar appeared centred on the fixation point and immediately started moving in one of eight directions at  $10^\circ \text{ s}^{-1}$ . The bar was  $20^\circ$  in length, and had a small, dim, red, gaussian blob ( $0.23 \text{ cd m}^{-2}$ ) in the centre. Direction and bar orientation were randomly interleaved across trials, and the monkey had to pursue the centre of the bar to within an accuracy of  $2^\circ$  to receive a liquid reward. Eye movements were monitored using the scleral search coil technique<sup>16</sup>. Both eye position and the eye velocity (obtained by analog differentiation, d.c. to 50 Hz,  $-20 \text{ dB per decade}$ ) were sampled at 1 kHz and stored to disk at 250 Hz for subsequent off-line analysis. To permit comparison across trials having different directions of target motion, the eye movement data were rotated relative to the target direction. Further details of animal preparation and data collection are given elsewhere<sup>27</sup>.

Received 11 September; accepted 11 December 2000.

1. Wallach, H. Uber visuell wahrgenommene Bewegungsrichtung. *Psychol. Forsch.* **20**, 325–380 (1935).
2. Wuergler, S., Shapley, R. & Rubin, N. “On the visually perceived direction of motion,” by Hans Wallach: 60 years later. *Perception* **11**, 1317–1367 (1996).
3. Marr, D. & Ullman, S. Directional selectivity and its use in early visual processing. *Proc. R. Soc. Lond. B.* **211**, 151–180 (1981).
4. Movshon, J. A. & Newsome, W. T. Visual response properties of striate cortical neurons projecting to area MT in macaque monkeys. *J. Neurosci.* **16**, 7733–7741 (1996).
5. Movshon, J. A., Adelson, E. H., Gizzi, M. S. & Newsome, W. T. The analysis of moving visual patterns. *Exp. Brain Res. Suppl.* **11**, 117–151 (1986).
6. Rodman, H. R. & Albright, T. D. Single-unit analysis of pattern-motion selective properties in the middle temporal visual area (MT). *Exp. Brain Res.* **75**, 53–64 (1989).
7. Stoner, G. R. & Albright, T. D. Neural correlates of perceptual motion coherence. *Nature* **358**, 412–414 (1992).
8. Albright, T. D. & Desimone, R. Local precision of visuotopic organization in the middle temporal area (MT) of the macaque. *Exp. Brain Res.* **65**, 582–592 (1987).
9. Maunsell, J. H. & Van Essen, D. C. Functional properties of neurons in middle temporal visual area of the macaque monkey. I. Selectivity for stimulus direction, speed, and orientation. *J. Neurophysiol.* **49**, 1127–1147 (1983).
10. Albright, T. D. Direction and orientation selectivity of neurons in visual area MT of the macaque. *J. Neurophysiol.* **52**, 1106–1130 (1984).
11. Pack, C. C. & Born, R. T. Latency of direction tuning in cortical area MT of alert macaque. *Soc. Neurosci. Abstr.* **25**, 673 (1999).
12. Newsome, W. T., Wurtz, R. H., Dürsteler, M. R. & Mikami, A. Deficits in visual motion processing following ibotenic acid lesions of the middle temporal visual area of the macaque monkey. *J. Neurosci.* **5**, 825–840 (1985).
13. Groh, J. M., Born, R. T. & Newsome, W. T. How is a sensory map read out? Effects of microstimulation in visual area MT on saccades and smooth pursuit eye movements. *J. Neurosci.* **17**, 4312–4330 (1997).
14. Lisberger, S. G. & Movshon, J. A. Visual motion analysis for pursuit eye movements in area MT of macaque monkeys. *J. Neurosci.* **19**, 2224–2246 (1999).
15. Krauzlis, R. J. & Lisberger, S. G. Temporal properties of visual motion signals for the initiation of smooth pursuit eye movements in monkeys. *J. Neurophysiol.* **72**, 150–162 (1994).
16. Robinson, D. A method of measuring eye movement using a scleral search coil in a magnetic field. *IEEE Trans. Biomed. Eng.* **10**, 137–145 (1963).
17. Lorençeau, J., Shiffar, M., Wells, N. & Castet, E. Different motion sensitive units are involved in recovering the direction of moving lines. *Vision Res.* **33**, 1207–1217 (1993).
18. Yo, C. & Wilson, H. R. Perceived direction of moving two-dimensional patterns depends on duration, contrast and eccentricity. *Vision Res.* **32**, 135–147 (1992).
19. Masson, G. S., Rybarczyk, Y., Castet, E. & Mestre, D. R. Temporal dynamics of motion integration for the initiation of tracking eye movements at ultra-short latencies. *Vis. Neurosci.* **17**, 753–767 (2000).
20. Beutter B. R. & Stone, L. S. Human motion perception and smooth eye movements show similar directional biases for elongated apertures. *Vision Res.* **38**, 1273–1286 (1998).
21. Hildreth, E. C. *The Measurement of Visual Motion* (MIT Press, Cambridge, Massachusetts, 1984).
22. Watanabe, T. & Cole, R. Propagation of local motion correspondence. *Vision Res.* **35**, 2853–2861 (1995).
23. Lidén, L. H. & Pack, C. C. The role of terminators and occlusion cues in motion integration and segmentation: A neural network model. *Vision Res.* **39**, 3301–3320 (1999).
24. Chey, J., Grossberg, S. & Mingolla, E. Neural dynamics of motion grouping: From aperture ambiguity to object speed and direction. *J. Opt. Soc. Am.* **14**, 2570–2594 (1997).
25. Wilson, H. R., Ferrera V. P. & Yo, C. A psychophysically motivated model for two-dimensional motion perception. *Vis. Neurosci.* **1**, 79–97 (1992).
26. Duncan, R. O., Albright, T. D. & Stoner, G. R. Occlusion and the interpretation of visual motion: perceptual and neuronal effects of context. *J. Neurosci.* **20**, 5885–5897 (2000).
27. Born, R. T., Groh, J. M., Zhao, R. & Lukasewicz, S. J. Segregation of object and background motion in visual area MT: effects of microstimulation on eye movements. *Neuron* **26**, 725–734 (2000).

**Acknowledgements**

We thank P. Abrams for technical assistance, and J. Assad and T. Watanabe for comments on a previous version of the manuscript. This work was supported by a McDonnell-Pew Cognitive Neuroscience grant to C.C.P., and grants from NIH/NEI and The Giovanni Armenise-Harvard Foundation for Scientific Research to R.T.B.

Correspondence and requests for materials should be addressed to C.C.P. (e-mail: cpack@hms.harvard.edu).